Multi-parametric Magnetic Resonance Imaging of Liver Regeneration in a Standardized Partial Hepatectomy Rat Model

Wen Shen (shenwen66happy@163.com)
Tianjin First Central Hospital, Tianjin Institute of imaging medicine
Caixin Qiu
Tianjin First Central Hospital, Tianjin Institute of imaging medicine
Shuangshuang Xie
Tianjin First Central Hospital, Tianjin Institute of imaging medicine
Yajie Sun
Tianjin First Central Hospital, Tianjin Institute of imaging medicine
Yongquan Yu
Weihai Central Hospital
Kun Zhang
Tianjin First Central Hospital, Tianjin Institute of imaging medicine
Xuyang Wang
Medical College of Nankai University
Jinxia Zhu
MR Collaboration, Siemens Healthcare Ltd
Robert Grimm
MR Application Predevelopment, Siemens Healthcare GmbH

Research Article

Keywords: magnetic resonance imaging (MRI), liver regeneration, hepatectomy, diffusion kurtosis imaging (DKI)

Posted Date: April 8th, 2022

DOI: https://doi.org/10.21203/rs.3.rs-1522104/v1

Abstract

Background : We aimed to evaluate the correlation between the pathological changes and multi-parameter MRI characteristics of liver regeneration (LR) in a standard partial hepatectomy (PH) rat model.

Methods : Seventy Sprague-Dawley rats were randomly divided into two groups: MR scan group (n = 14) and pathologic analysis (PA) group (n = 56). All 14 rats in the MR group underwent liver T1 mapping, T2 mapping, and diffusion kurtosis imaging (DKI) before and the 1st, 2nd, 3rd, 5th, 7th, 14th, and 21st day after 70% hepatectomy. Seven rats in the PA group were euthanized at each time point to determine Ki-67 indices, hepatocyte size (HTS), and steatosis grade.

Results : Liver T1 and T2 values increased to maximum on day 2 ($P < .001$ vs. baseline), D and K values decreased to minimum on day 3 and 2, respectively ($P < .001$ vs. baseline), then all parameters returned to baseline gradually. Hepatocyte Ki-67, hepatocyte size and steatosis grade initially increased after surgery ($P < 0.05$ vs. baseline), followed by a gradual decline over time. Both T2 and K values correlated well with Ki-67 indices (r = 0.756 and -0.807, respectively; both $P < .001$) and steatosis grade (r = 0.814 and -0.725, respectively; both $P < .001$), moderate with HTS (r = 0.640 and -0.562, respectively; both $P < .001$).

Conclusions : PH induced liver changes that can be observed on MRI. The MRI parameters correlate with the LR activity and allow monitoring of LR process.

Introduction

Partial hepatectomy (PH) is a surgical treatment for liver tumors and a necessary surgical procedure for living donor liver transplantation [1]. Residual liver regeneration is closely related to the prognosis of liver tumor patients, donors, and recipients. Although PH has been widely used in clinical practice and is a relatively safe procedure, patients still face the risk of surgical failure due to liver regeneration failure [2]. Therefore, finding an appropriate method to monitor liver regeneration is of great concern to hepatobiliary surgeons. At present, computed tomography or magnetic resonance imaging (MRI) measurement of liver volume to monitor liver regeneration is a commonly used method in clinical practice [3–6]. However, volume recovery may be overestimated and cannot reflect the microscopic changes of liver parenchyma [6]. Previous studies have reported that hypertrophy and hepatocyte division contribute to liver regeneration [7]. In this process, the number of residual hepatocytes, hepatocyte size, tissue structure, and material metabolism changed significantly [8]. MRI offers a non-invasive option for assessing biomarkers associated with pathophysiologic changes. MR T1 mapping and T2 mapping scanning can assess water molecule content, collagen fiber deposition, inflammation, and lipid infiltration of the tissue, corresponding to possible changes during liver regeneration [9, 10]. Diffusion kurtosis imaging (DKI) is sensitive to tissue microstructure and conducive to reflecting the actual situation in tissues, providing an opportunity to gain insights into the state of liver diffusivities and tissue microstructural complexity [11–14]. Published studies have investigated the association between a single MRI feature and liver

regeneration, but few have comprehensively assessed liver regeneration and their associations pathologically and radiologically [15–17].

In this study, we used multi-parametric MRI to longitudinally observe liver changes in a standardized rat model after 70% PH. Our purpose was to determine whether multi-parametric MRI values from T1 and T2 mapping and DKI could be used to correlate microscopic liver regeneration changes to residual liver regeneration indices, and thus to lay an experimental basis for clinicians to find a non-invasive method for assessing liver regeneration.

Materials And Methods

Animals

A total of 70 male Sprague-Dawley rats aged 7 to 8 weeks and weighing 260 ± 30g were obtained (China Food and Drug Control Research Institute, Beijing, China). Animals were housed in the animal facility of the Key Laboratory of Organ Transplantation of Tianjin with unrestricted access to standard chow and water. All experiments were approved by the NANKAI University Animal Experimentation Ethics Committee and performed according to the University's animal care guidelines. Rats were randomly divided into two groups: an MR scan (MR) group (n = 14) and a pathologic analysis (PA) group (n = 56). The MR group was further divided into a 70% PH subgroup (MRph, n = 7) and a control subgroup (MRctrl, n = 7). Before surgery, all 14 rats in the MR group underwent MR imaging, and a random 7 of the 56 rats in the PA group were euthanized for pathologic analysis to establish baseline values. The 7 rats in the MRph subgroup and the 56 rats in the PA group underwent a 70% PH, and the 7 rats in the MRcrtl subgroup underwent a sham operation. MR scan group underwent liver T1 mapping, T2 mapping, and DKI examinations before and on the 1st, 2nd, 3rd, 5th, 7th, 14th, and the 21st day after surgery. The PA group, 56 rats in total, randomly selected seven with 70% PH at each corresponding time point above for pathologic analysis, including Ki-67 indices, hepatocyte diameter, and steatosis grade (Fig. 1).

Anesthesia and surgical procedures

The surgical procedures were performed under inhalation anesthesia. Induction was performed in a glass box with a mixture of 2% isoflurane in oxygen (1.0 L/min) (Ruiwode; Shenzhen, China). During surgery, anesthesia was maintained with 2% isoflurane in oxygen through a mask covering the animal's mouth and nose. The animal placed supine on an operating plate underwent a midline laparotomy, and the liver was freed from its ligaments. For the MRph and PA groups, the common pedicle of the left lateral and median lobes was ligated with a 4-0 suture, and the lobes were resected. The abdomen was then closed with a 3-0 suture. For the MRcrtl group, the left lateral and medial lobes were freed from ligaments. The abdomen was then closed with a 3-0 suture.

Magnetic resonance imaging

All the rats underwent MRI examinations on a 3T MR scanner (MAGNETOM Prisma, Siemens Healthcare, Erlangen, Germany) with an 8-channel animal coil (Chenguang, Shanghai, China). The rats were anesthetized with isoflurane inhalation and placed in a prone position to reduce respiratory motion. T1 weighted imaging (T1WI) was performed for liver segmentation. The T1 mapping was acquired using a 3D gradient echo sequence with the volumetric interpolated breath-hold examination (VIBE) sequence with a dual-flip-angle method. Sequence parameters were: repetition time (TR) = 6.30 ms, echo time (TE) = 2.88 ms, Flip angles = 3° and 15°, field of view (FOV) = 120×98 mm^2, slice thickness = 3 mm, matrix =192 × 156, voxel size = 0.6×0.6×3 mm^3, bandwidth = 300 Hz/px, acquisition time = 2 min 27sec. T2 mapping was acquired using a multi-echo spin echo sequence, with following parameters: TR = 2000 ms, 6 TEs = 13/26/39/52/65/78 ms, FOV = 120×120 mm^2, slice thickness = 3 mm, matrix = 128×96, reconstructed voxel size = 0.5×0.5×3 mm^3, bandwidth = 201 Hz/px, acquisition time = 4 min 50 sec. DKI was performed using a free-breathing single-shot EPI sequence with the following parameters: TR = 2300 ms, TE = 74 ms, FOV = 120×98 mm^2, slice thickness = 3 mm, matrix = 128×98, reconstructed voxel size = 0.5 × 0.5 × 3 mm^3, acquisition time = 4 min 43 sec. Five b-values (0, 500, 1000, 1500, and 2000 s/mm^2) were applied in 3 directions.

MRI liver volume measurement

Regions of interest (ROI) were manually drawn using T1WI by two independent blinded examiners. The liver volume was measured using software from an IQQA-3D-Liver workstation (EDDA Technologies, USA), allowing quantitative ROI analysis. Liver volume was determined by summing the manual segmentation from each slice.

Imaging data analysis

Parametric T1 and T2 maps were generated inline after data acquisition. DKI data were post-processed using a prototype software (MR Body Diffusion Toolbox, Siemens Healthcare, Erlangen, Germany), the DKI-derived parameters (D and K values) were obtained. Five ROIs measuring 12~15mm^2 were drawn on the residual liver to measure the T1, T2, D, and K values while avoiding large vessels, artifacts, and the liver border. The average of the five values was used as the final ROI. Two experienced radiologists analyzed all images in a blinded manner.

Histology and immunohistochemistry

Liver tissue was fixed in a buffered 4% formaldehyde solution, embedded in paraffin, stained with hematoxylin-eosin (HE) and Sirius red using standard histologic techniques. Liver samples were stained with HE to observe the hepatic pathologic structure and determine the hepatocyte size and steatosis grade. All pathologic specimens were reviewed by an experienced pathologist. Hepatocyte size (diameter)

was determined by measuring ten hepatocytes in high-power fields (×400) [18]. The grade of steatosis is based on the proportion of hepatocytes containing visible lipid and is expressed semi-quantitatively on a scale of 0-3 (S0, < 5%; S1, 5%-33%; S2, > 33%-66%; S3, > 66%) [19]. Immunohistochemical staining was performed to determine the proliferative index Ki-67 (1:100; Abcam, Cambridge, UK). The number and ratio of Ki-67-positive cells were determined by manual counting in five high-power random fields (×400) per slide.

Statistics

Statistical analysis was performed on SPSS Version 22 for Mac (SPSS 22; IBM Company, Chicago, IL). The normal distribution of MR parameters in the MRph and MRctrl groups was tested using the Shapiro-Wilk test. Repeated measure one-way ANOVAs were used to compare MR parameters' difference between two groups at different time points. The liver volume and pathologic indices at different time points were compared by one-way ANOVAs. The correlations between MR and liver regeneration parameters were determined using Pearson correlation coefficient analysis or Spearman's rank correlation analysis. The threshold of significance was set to 0.05.

Results

MR parameters analysis

Representative parametric mapping of T1, T2, D, and K for one rat with PH are shown in Fig.2A. The means and standard deviations for the T1, T2, D, and K changes and comparisons across different time points are listed in Table 1. All MR parameters, including T1, T2, D, and K values, showed significant changes immediately after PH and then gradually recovered towards the preoperative baseline with the end of regeneration.

Both T1 and T2 values significantly increased post-PH and increased to the maximum on day 2 (both $P <$ .001 vs. baseline), and then returned towards their baseline values. T1 values recovered to the preoperative level on day 14 ($P >$ .05 vs. baseline), T2 values recovered to the preoperative level on day 21 ($P >$ .05). The T2 values were significantly different from the adjacent time points on days 1, 3, 7, and 14 (all $P <$ .001 vs. adjacent time points). T1 values were significantly higher than the MRctrl group on days 1, 2, 3, and 7 (all $P <$ .05) (Fig. 2B). T2 values were significantly higher compared to the MRctrl group for all time points except day 21 (all $P <$ .001) (Fig. 2B).

Both D and K values significantly decreased post-PH, D values decreased to a minimum value on day 3 ($P <$ .001 vs. baseline), then gradually increased. The K values decreased to a minimum value on day 2 ($P <$ .001), then gradually increased, and the value increased to the baseline value on day 7 and demonstrated no significant difference compared to baseline by day 7 ($P >$ .05). D values were significantly higher compared to the MRctrl group for all time points (all $P <$ .05) (Fig. 2B). K values were considerably higher than the MRctrl group on days 1~5 (all $P <$ .05) (Fig. 2B).

Intraclass correlations in the MRph group for T1, T2, D, and K were 0.856, 0.931, 0.948, and 0.851, respectively .

Liver volume analysis

Post-PH, liver volume recovered rapidly, and increased significantly on postoperative days 1~5, demonstrating a significant difference compared to the adjacent time points (all $P < .001$) (Table 2). The growth rate of liver volume began to slow down on postoperative days 7, and the liver volume demonstrated no significant difference compared to the adjacent time points ($P > .05$). On day 21, liver volume was approximately 80% of preoperative liver volume (Table 2).

Histopathological analysis

There were notable morphological alterations over the time course of liver regeneration. The cytoplasm of hepatocytes in the remnant liver was swollen due to fluid and lipid infiltration, indicating hepatocyte hypertrophy after PH. Fat quantification showed that steatosis of liver remnant tissue was most apparent (S3 stage) on day 1, and still evident on days 2 to 3 (S2 stage). It decreased significantly on days 5 to 7 (S1 stage) and recovered to the preoperative level on day 14 (S0 stage) (Fig 3A). Post-PH, hepatocyte size was significantly larger compared with the baseline on day 1 and reached a maximum ($P < .001$), then decreasing to near-baseline by day 7 ($P > .05$) (Fig. 3B, Table 2). The representative immunohistochemical images depict Ki-67 positive hepatocytes after PH (Fig. 3A). Ki-67 indices were significantly higher post-PH than baseline, reaching a maximum on day 2 ($P < .001$) and returning to near-baseline by day 14. No significant increase in positive hepatocytes was observed in the baseline data (Table 2).

Correlation analysis

Both T2 and K values correlated with liver regeneration-related indices (Table 3, Fig. 4). T2 values showed a strong correlation with liver volume (r = -0.764; $P < .001$), steatosis grade (r = 0.814; $P < .001$), Ki-67 indices (r = 0.765; $P < .001$), and a moderate correlation with hepatocyte size (r = 0.640; $P < .001$). K values had better correlations with Ki-67 indices (r = -0.807; $P < .001$), and steatosis grade(r = -0.725; $P < .001$) than with liver volumes (r = 0.595; $P < .001$), and hepatocyte size (r = -0.562; $P < .001$). A moderate correlation was observed between T1 values and liver volume (r = -0.481; $P < .001$), Ki-67 indexes (r = 0.444; $P < .001$), steatosis grade (r = 0.476; $P < .001$), and hepatocyte size (r = 0.472; $P < .001$). However, D values were only moderately correlated with hepatocyte size (r = -0.469; $P < .001$) and were not or were weakly correlated with other parameters.

Discussions

This study demonstrated that the multi-parametric MRI monitoring of liver regeneration in the standard rat model is feasible. Moreover, the regeneration process of the residual liver had a good correlation between MRI parameters and histopathological characteristics. These significant relationships have the potential to reveal and elucidate the complex process of residual liver regeneration and have the possible use of these parameters as non-invasive biomarkers to monitor liver regeneration.

Previous studies concluded that liver regeneration after PH is mainly contributed by hepatocyte proliferation [20]. However, Miyaoka et al.[7] found that the volume growth of residual liver after PH was caused by both hypertrophy and proliferation of hepatocytes. Ki-67 immunostaining can mark liver cells in the mitotic stage of liver tissue and has been widely used in animal studies on liver regeneration [7, 16, 17, 21, 22]. In this study, we found that both hepatocyte diameter and Ki-67 proliferation indices significantly increased after PH, indicating that both processes are involved in liver regeneration, in consistent with Miyaoka's studies [7]. The liver volume and hepatocyte diameter increased significantly on day 1. A large number of Ki-67 positive cells were also observed, suggesting that residual liver tissue could start regeneration quickly to compensate for the loss of liver to maintain normal function. The liver volume continued to increase on day 2, and Ki-67 positive cells also continued to increase and reached the maximum, indicating the regeneration peak, which was consistent with a previous animal study [21]. The third day was a turning point when the regeneration rate decreased, and the number of Ki-67 positive cells started to fall. The hepatocyte diameter returned to the baseline level on day 7, and Ki-67 positive cells also reduced to a shallow level, demonstrating that the liver regeneration reached a plateau on day 7, followed by slow growth until the end of regeneration, which agrees with a study by Hockings et al.[17] These findings may have important implications for future research on the timing of drug intervention in liver regeneration. In addition, interestingly, we found that the corresponding MR parameters also showed a similar trend; T1 and T2 values increased significantly on day 1, reached the maximum on day 2, and began to decline on day 3. K value began to decrease on day 1, came to the minimum on day 2, and increased on day 3. It returned to the preoperative level on day 7, and the subsequent changes were not significant. These results indicate that MR parameters can reflect the changing trend of the liver regeneration process.

In our study, we measured T1 and T2 values of liver parenchyma before and after surgery, and the preoperative baseline values we measured were basically in keeping with a previous study [16]. In addition, we found that T1 and T2 values increased first and then gradually recovered to baseline, which was also in line with the results of Hockings et al. [17]. However, these published studies on rats assessed T1 and T2 values post-PH without detailed data on corresponding pathological results. The increased T1 values reflect the tissue water accumulation due to edema and inflammation after PH [10]. While T2 values are sensitive to an increase in hepatocyte water content and free water fractions [9]. Our histological findings found that significant swelling and steatosis occurred in the first few days after PH and then gradually decreased, based on the observed changes in hepatocyte size throughout the study. Moreover, it has long been known that liver regeneration leads to the rapid accumulation of intracellular lipids in mouse models of PH, suggesting that liver steatosis is an an essential liver regeneration process [21]. Cassinotto et al.[23] have shown a correlation between liver T2 values and the degree of liver

steatosis, which is in good agreement with our results. Therefore we speculated that the significant increase in T2 values after PH results from an increase in residual hepatic steatosis and water content. Increases in fat content significantly decrease T1 values, reducing the ability of the increase in postoperative water content to prolong T1. This may have interfered with an increase in postoperative T1 values in our study. Moreover, we also found that both T1 and T2 values were correlated with hepatocyte size and Ki-67 indices. Potentially elevated cellular hypertrophy resulting from swollen hepatocytes, a higher number of proliferating, and enhanced lipid content might account for the increased T1 and T2 values in post-PH livers. These results indicate that both T1 and T2 values can be used to monitor the dynamic changes of the liver regeneration process after PH.

Previously, Eberhardt et al.[16] used apparent diffusion coefficients (ADC) derived from conventional diffusion-weighted imaging to evaluate changes in liver parenchyma after PH, and found that the ADC of liver parenchyma decreased after PH. However, ADC is calculated using a monoexponential analysis, which assumes Gaussian behavior of water diffusion. DKI provides a model to quantify non-Gaussian water diffusion. It is more sensitive to the states of liver diffusivities and tissue microstructural complexity compared to standard DWI. The parameter D derived from DKI represents the corrected apparent diffusion. The D values of tissues is affected by cell perimeter length, cell density, size, and permeability, and a study showed that the cell perimeter length is the most important factor [24–25]. In this work, the D values were significantly decreased at all time points, indicating cellular hypertrophy with limited diffusivity. Moreover, the correlation analysis showed that D value had a moderate negative correlation with hepatocyte size. Thus, the decrease in D may be explained by the increases in cell perimeter length due to cellular hypertrophy. K values are a measure of the complexity and heterogeneity of the cell microenvironment. K values were significantly reduced after PH, in line with the results of Sheng et al.[26] Residual hepatic sinusoids dilate, the arrangement of the sieve plate disappears after PH, exposing the surface of hepatic parenchymal cells to the portal vein, resulting in a relative reduction in tissue complexity [27]. A reduction in tissue complexity may explain our observation that K values decreased in the early postoperative period. However, hepatocellular hypertrophy often affects the microstructure, which may not be explained by a simple Gaussian or restricted diffusion model. Further studies are necessary. In addition, the correlation analysis showed that K value had a good correlation with liver regeneration-related indices (liver volume, steatosis grade, Ki-67 indices, and hepatocyte size), indicating the potential value of K values in reflecting liver regeneration processes.

This study had several limitations. First, the kinetics of regeneration differs between humans and rodents, and the results of this study may not fully represent human liver regeneration after PH. Second, imaging animals were not subjected to histological analysis to achieve dynamic and continuous acquisition of MR parameter data. Third, this study analyzed liver regeneration after hepatectomy in normal liver, but liver regeneration in the context of other liver conditions is different.

Conclusions

This study used multi-parameter MRI, including the T1 and T2 mapping and DKI, to longitudinally observe rat liver regeneration after PH. The MR parameters showed a consistent change trend with pathological indicators, and correlated with liver regeneration-related indices. Multi-parametric MRI can detect microstructural changes in the residual liver after PH. These techniques might provide non-invasive, sensitive, and quantitative tools for the characterization of residual liver regeneration processes.

Abbreviations

MRI: magnetic resonance imaging; PH: partial hepatectomy; DKI: diffusion kurtosis imaging; PA: pathologic analysis; ROI: regions of interest; HE: hematoxylin-eosin; HTS: Hepatocyte size; LR: liver regeneration; ADC: apparent diffusion coefficients.

Declarations

Ethics approval and consent to participate

The animal experiments complied with the ARRIVE guidelines and the experimental protocols were performed after approval and in accordance with the guidelines set by the Medical Ethics Committee of Nankai University, and the approval number was 2021-SYDWLL-000475.

Consent for publication

Not applicable.

Availability of data and materials

The datasets used and analysed during the current study are available from the corresponding author on reasonable request.

Author contributions

Caixin Qiu: designed the study, carried out experiments; analyzed the data, and drafted the manuscript; Shuangshuang Xie: carried out experiments, analyzed the data; Yajie Sun,Yongquan Yu,Kun Zhang and Xuyang Wang: carried out experiments; Jinxia Zhu and Robert Grimm contributed with MRI protocol and revised the manuscript; Wen Shen: designed the study, revised the manuscript. All authors reviewed the manuscript.

Competing interests

The authors declare that they have no competing interests.

Funding

This study has received funding by the National Natural Science Foundation of China (81901710 and 81873888) and Science and Technology Fund of Tianjin (QN20024). Tianjin Key Medical Discipline (Specialty) Construction Project.

Acknowledgments

None.

References

1. Clavien PA, Oberkofler CE, Raptis DA et al. What is critical for liver surgery and partial liver transplantation: size or quality? HEPATOLOGY 2010;52:715-729.
2. van den Broek MA, Olde DS, Dejong CH et al. Liver failure after partial hepatic resection: definition, pathophysiology, risk factors and treatment, LIVER INTERNATIONAL 2008;28:767-780.
3. Tsomaia K, Patarashvili L, Karumidze N et al. Liver structural transformation after partial hepatectomy and repeated partial hepatectomy in rats: A renewed view on liver regeneration, World J Gastroenterol 2020;26:3899-3916.
4. Guglielmi A, Ruzzenente A, Conci S et al. How much remnant is enough in liver resection? Dig Surg 2012;29:6-17.
5. de Graaf W, Bennink RJ, Heger M et al. Quantitative assessment of hepatic function during liver regeneration in a standardized rat model, JOURNAL OF NUCLEAR MEDICINE 2011;52:294-302.
6. Nagino M, Ando M, Kamiya J et al. Liver regeneration after major hepatectomy for biliary cancer, Br J Surg 2001;88:1084-1091.
7. Miyaoka Y, Ebato K, Kato H et al. Hypertrophy and unconventional cell division of hepatocytes underlie liver regeneration, CURRENT BIOLOGY 2012;22:1166-1175.
8. Siu J, McCall J, Connor S. Systematic review of pathophysiological changes following hepatic resection, HPB (Oxford) 2014;16:407-421.
9. Hoffman DH, Ayoola A, Nickel D et al. T1 mapping, T2 mapping and MR elastography of the liver for detection and staging of liver fibrosis, Abdom Radiol (NY) 2020;45:692-700.
10. Taylor AJ, Salerno M, Dharmakumar R et al. T1 Mapping: Basic Techniques and Clinical Applications, JACC Cardiovasc Imaging 2016;9:67-81.
11. Sheng RF, Yang L, Jin KP et al. Assessment of liver regeneration after associating liver partition and portal vein ligation for staged hepatectomy: a comparative study with portal vein ligation, HPB (Oxford) 2018;20:305-312.
12. Rosenkrantz AB, Padhani AR, Chenevert TL et al. Body diffusion kurtosis imaging: Basic principles, applications, and considerations for clinical practice, JOURNAL OF MAGNETIC RESONANCE IMAGING 2015;42:1190-1202.
13. Goshima S, Kanematsu M, Noda Y et al. Diffusion kurtosis imaging to assess response to treatment in hypervascular hepatocellular carcinoma, AJR Am J Roentgenol 2015;204:W543-W549.

14. Jensen JH, Helpern JA, Ramani A et al. Diffusional kurtosis imaging: the quantification of non-gaussian water diffusion by means of magnetic resonance imaging, MAGNETIC RESONANCE IN MEDICINE 2005;53:1432-1440.
15. Sheng RF, Wang HQ, Jin KP et al. Histogram analyses of diffusion kurtosis indices and apparent diffusion coefficient in assessing liver regeneration after ALPPS and a comparative study with portal vein ligation, JOURNAL OF MAGNETIC RESONANCE IMAGING 2018;47:729-736.
16. Eberhardt C, Wurnig MC, Wirsching A et al. Prediction of small for size syndrome after extended hepatectomy: Tissue characterization by relaxometry, diffusion weighted magnetic resonance imaging and magnetization transfer, PLoS One 2018;13:e192847.
17. Hockings PD, Roberts T, Campbell SP et al. Longitudinal magnetic resonance imaging quantitation of rat liver regeneration after partial hepatectomy, TOXICOLOGIC PATHOLOGY 2002;30:606-610.
18. Matsuo K, Murakami T, Kawaguchi D et al. Histologic features after surgery associating liver partition and portal vein ligation for staged hepatectomy versus those after hepatectomy with portal vein embolization, SURGERY 2016;159:1289-1298.
19. Kleiner DE, Brunt EM, Van Natta M et al. Design and validation of a histological scoring system for nonalcoholic fatty liver disease, HEPATOLOGY 2005;41:1313-1321.
20. Palmes D, Spiegel HU. Animal models of liver regeneration, BIOMATERIALS 2004;25:1601-1611.
21. Wirsching A, Eberhardt C, Wurnig MC et al. Transient steatosis assessed by magnetic resonance imaging predicts outcome after extended hepatectomy in mice, AMERICAN JOURNAL OF SURGERY 2018;216:658-665.
22. Meier M, Andersen KJ, Knudsen AR et al. Liver regeneration is dependent on the extent of hepatectomy, JOURNAL OF SURGICAL RESEARCH 2016;205:76-84.
23. Cassinotto C, Feldis M, Vergniol J et al. MR relaxometry in chronic liver diseases: Comparison of T1 mapping, T2 mapping, and diffusion-weighted imaging for assessing cirrhosis diagnosis and severity, EUROPEAN JOURNAL OF RADIOLOGY 2015;84:1459-1465.
24. Le Bihan D. Apparent diffusion coefficient and beyond: what diffusion MR imaging can tell us about tissue structure, RADIOLOGY 2013;268:318-322.
25. Sheng RF, Jin KP, Yang L et al. Histogram Analysis of Diffusion Kurtosis Magnetic Resonance Imaging for Diagnosis of Hepatic Fibrosis, KOREAN JOURNAL OF RADIOLOGY 2018;19:916-922.
26. Morsiani E, Aleotti A, Ricci D. Haemodynamic and ultrastructural observations on the rat liver after two-thirds partial hepatectomy, JOURNAL OF ANATOMY 1998;192 (Pt 4):507-515.

Tables

Table 1

MR parameters of MRph and MRctrl groups changes and comparison across different time points.

Time Point	T1 (ms)		T2 (ms)		D (× 10^{-3} mm^2/s)		K	
	MRph	MRctrl	MRph	MRctrl	MRph	MRctrl	MRph	MRctrl
Baseline	916.0 ± 62.9	921.8 ± 8.4	35.8 ± 1.4	35.4 ± 0.6	1.60 ± 0.09	1.54 ± 0.04	0.68 ± 0.02	0.68 ± 0.04
Day 1	1031.3 ± 84.2	943.7 ± 31.7	48.8 ± 3.2*#	36.1 ± 1.2	1.30 ± 0.17*#	1.64 ± 0.04	0.55 ± 0.07*#	0.65 ± 0.02
Day 2	1081.8 ± 85.2*	954.0 ± 54.7	50.00 ± 3.7*	36.1 ± 0.8	1.21 ± 0.14*	1.61 ± 0.05	0.46 ± 0.06*	0.64 ± 0.02
Day 3	1011.74± 36.7	941.9 ± 62.1	44.6 ± 3.2*#	36.4 ± 1.1	1.14 ± 0.10*	1.63 ± 0.06	0.54 ± 0.06*	0.65 ± 0.02
Day 5	1038.5 ± 86.1	958.7 ± 89.9	46.1 ± 1.6*	34.5 ± 0.6#	1.15 ± 0.17*	1.64 ± 0.05	0.60 ± 0.05*	0.67 ± 0.03
Day 7	1050.1 ± 61.3*	937.8 ± 34.6	41.7 ± 3.2*#	34.6 ± 1.3	1.16 ± 0.18*	1.60 ± 0.03	0.67 ± 0.03	0.66 ± 0.05
Day 14	955.3 ± 141.8#	895.3 ± 58.8	39.7 ± 2.7*	36.0 ± 2.3#	1.24 ± 0.09*	1.62 ± 0.13	0.66 ± 0.03	0.65 ± 0.02
Day 21	918.8 ± 68.4	902.1 ± 64.9	37.1 ± 3.6#	34.3 ± 1.8#	1.33 ± 0.12*	1.61 ± 0.03	0.66 ± 0.04	0.63 ± 0.03
F	3.947	1.469	22.587	3.300	8.771	2.213	19.802	2.225
P	0.04	0.201	< .001	0.006	< .001	0.063	< .001	0.052

Note: Data are shown as mean and standard deviation. D, corrected apparent diffusion; K, kurtosis; * Data are significantly different compared to baseline. # Data are significantly different compared to the adjacent time points.

Table 2

Changes and comparison of liver volume and pathologic parameters related to liver regeneration

Time point	LV（cm^3）	HTS (um)	Ki-67 indices (%)
Baseline	10.23±0.56	19.73±1.07	4.61±1.08
Day 1	4.84±0.42*#	26.67±2.09*#	31.78±1.16*#
Day 2	6.06±0.61*#	25.69±1.06*	44.52±2.02*#
Day 3	7.01±0.73*#	24.08±1.62*	19.22±1.39*#
Day 5	7.87±0.66*#	24.16±1.48*	11.38±1.33*#
Day 7	8.31±0.56*	22.29±2.90	8.51±0.78*#
Day 14	8.79±0.33*	22.26±1.72	5.08±1.29#
Day 21	9.21±0.65*	21.56±1.35	4.35±0.98
F	115.080	11.791	903.031
P	**< .001**	**< .001**	**< .001**

Note: Data are shown as mean and standard deviation. LV, Liver volume; HTS, Hepatocyte size. * Data are significantly different compared to baseline. # Data are significantly different compared to the adjacent time points

Table 3

Correlations between MR and pathologic analysis parameters

Characteristic	T1(ms)		T2(ms)		D (×$10^{-3}$$mm^2$/s)		K	
	r	*P* value	r	*P* value	r	*P* value	r	*P* value
LV (cm^3)	-0.481	**< .001**	-0.764	**< .001**	0.364	.006	0.595	**< .001**
Ki-67 (%)	0.444	**< .001**	0.765	**< .001**	-0.208	.124	-0.807	**< .001**
Hepatocyte size (μm)	0.472	**< .001**	0.640	**< .001**	-0.469	**< .001**	-0.562	**< .001**
Steatosis grade	0.476	**< .001**	0.814	**< .001**	-0.337	.011	-0.725	**< .001**

Significant results are in bold.

D, corrected apparent diffusion; K, kurtosis; LV, Liver volume.

r =: |0.0-0.2|, very weak to negligible correlation; |0.2-0.4|, weak correlation; |0.4-0.7|, moderate correlation; |0.7-0.9|, strong correlation; and |0.9-1.0|, very strong correlation.

Figures

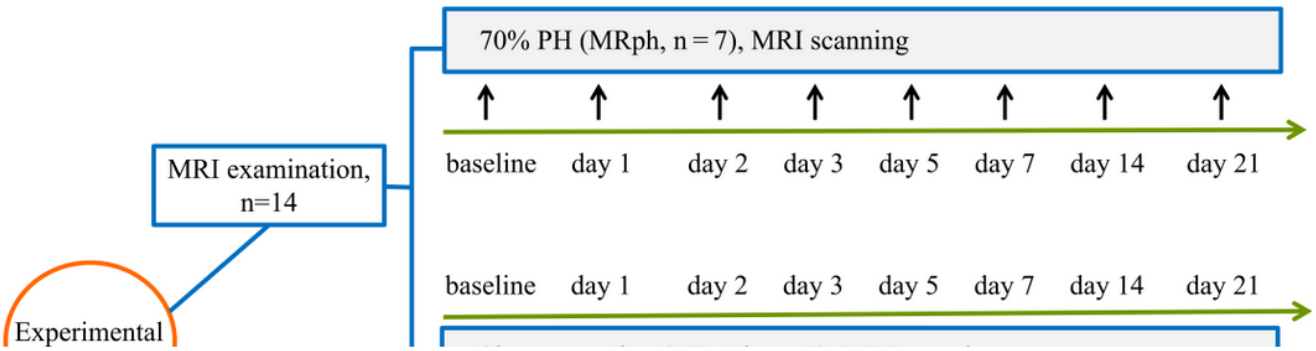

Figure 1

The experimental protocol in this study. PH = partial hepatectomy.

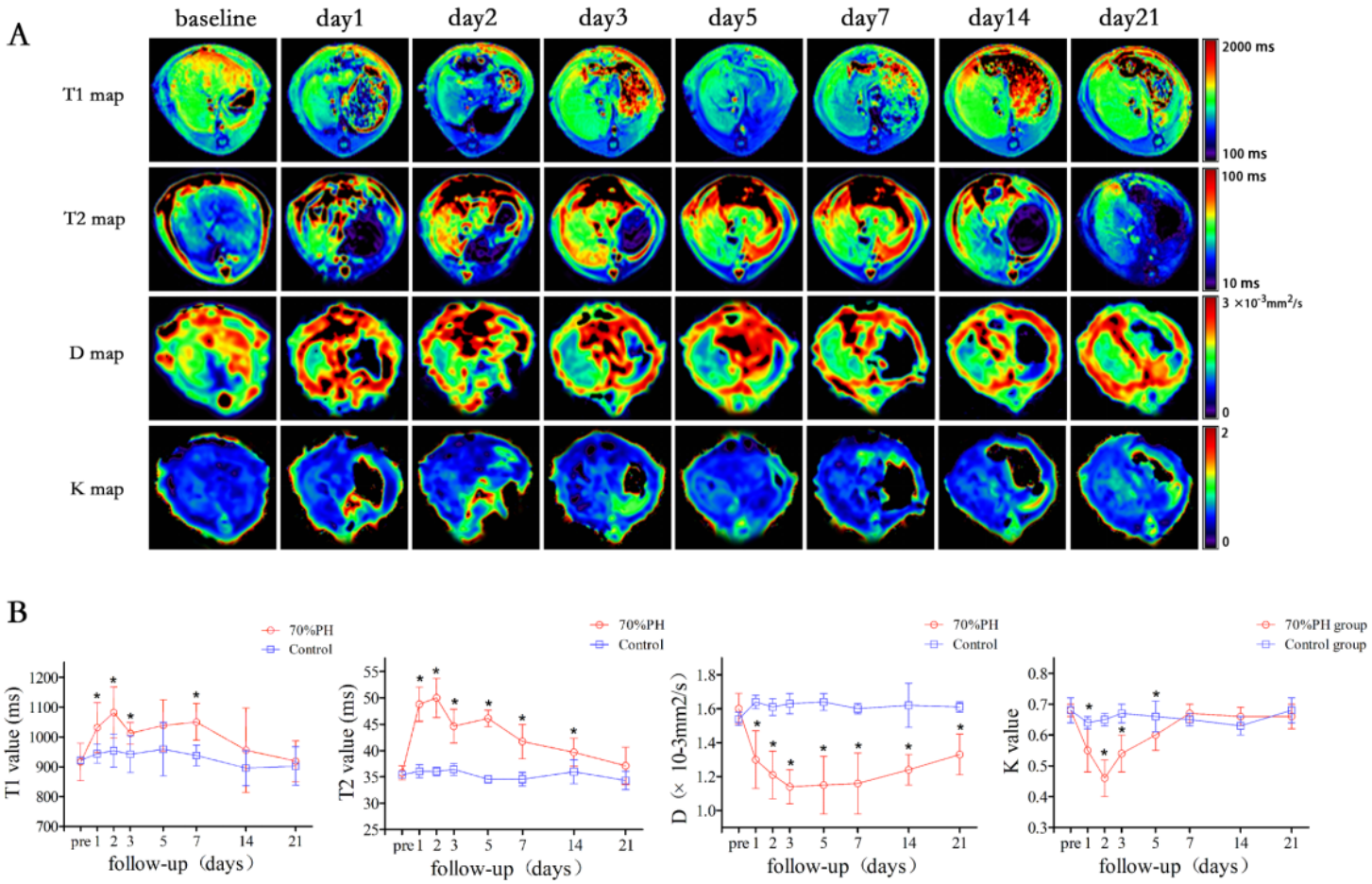

Figure 2

A, representative cropped T1, T2, D, and K parametric maps of the regenerating liver from preoperative and postoperative rats; B, Changes of T1,T2,D and K values after PH. Error bars represent the standard deviations of the mean values. * significant changes compared with control group.

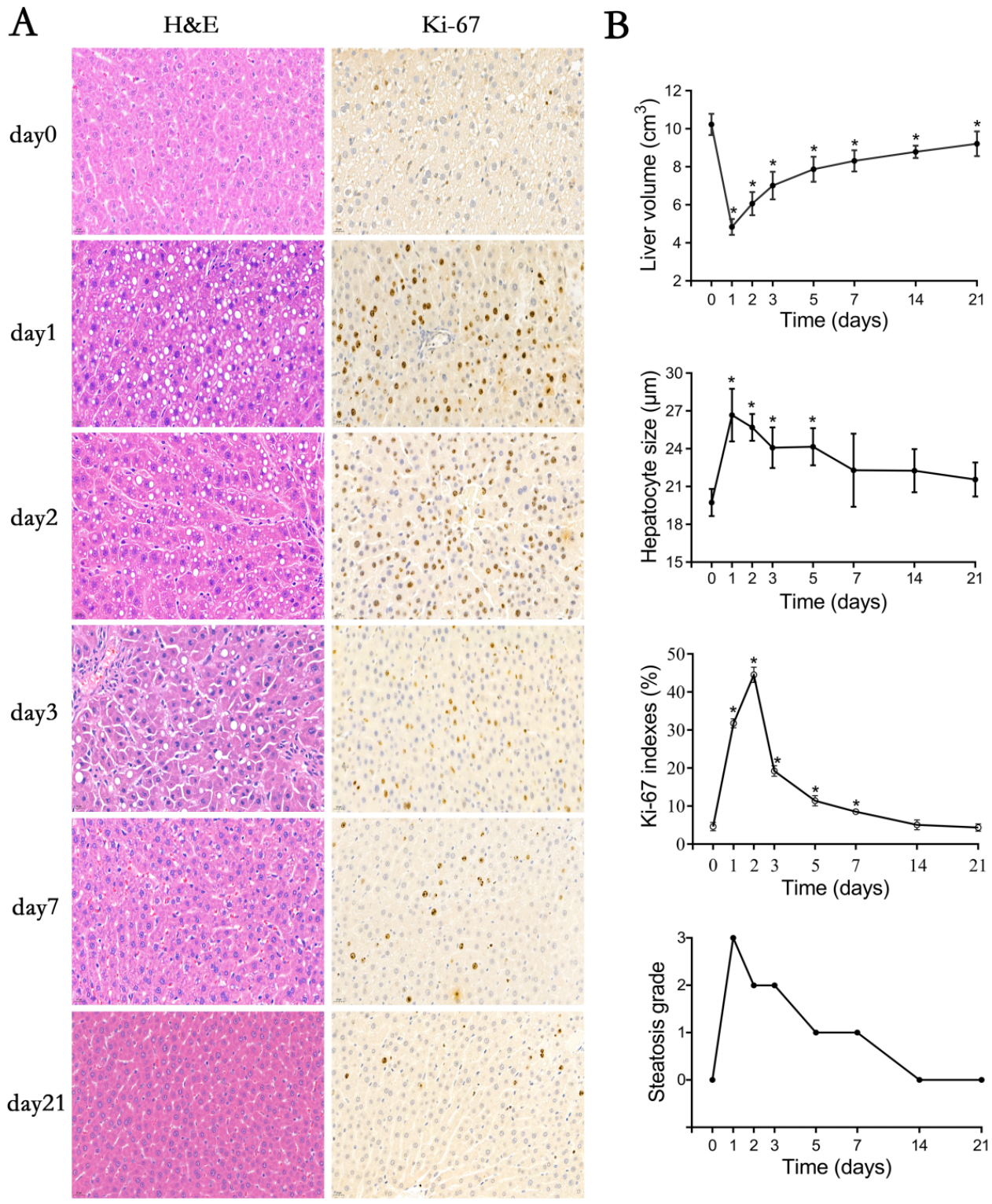

Figure 3

Characteristics of liver tissue preoperative and postoperative. A, Hematoxylin-eosin staining (×400) and Ki-67 proliferation activity staining (×400). B, Liver volume growth, hepatocyte size, Ki-67 proliferation indexes, and steatosis grade. Error bars represent the standard deviations of the mean values. * Data are significantly different compared to baseline.

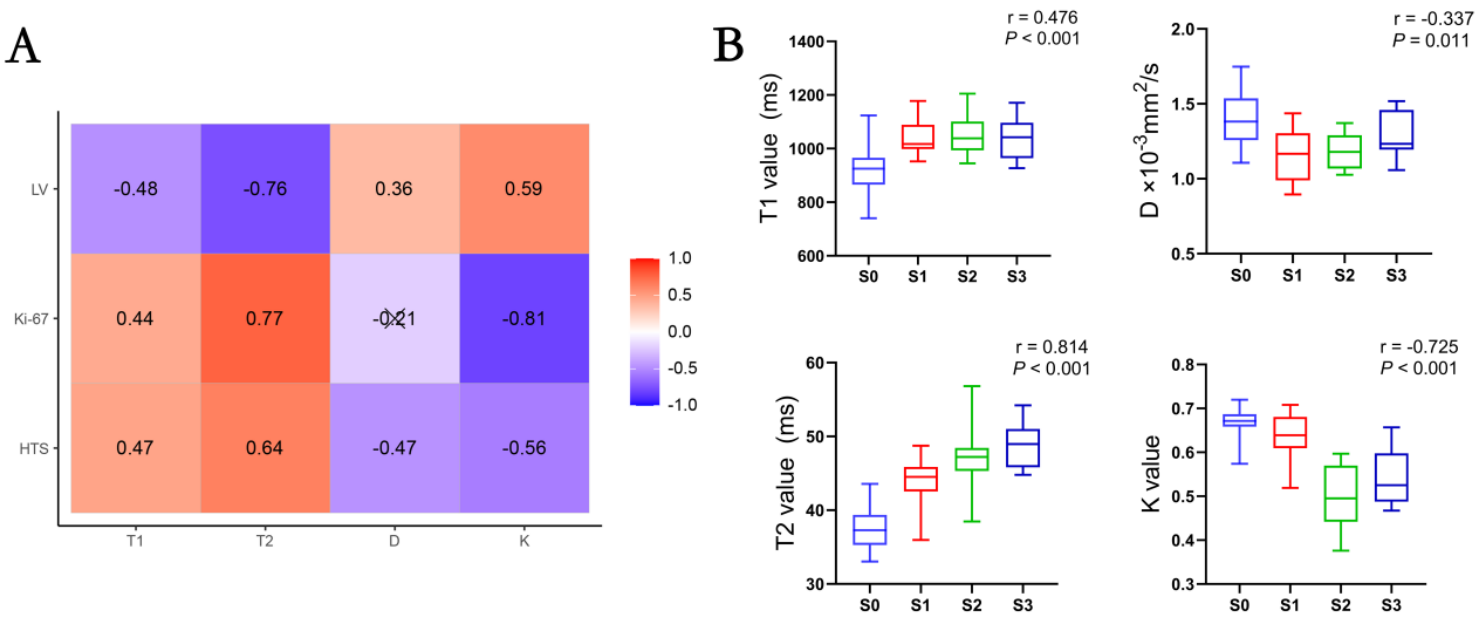

Figure 4

A, Correlation heatmaps for quantitative MR imaging parameters and pathological measurements related to liver regeneration. LV, liver volume; HTS, hepatocyte size; B, Spearman correlation between magnetic resonance imaging (MRI) parameters and steatosis grade.